PERFORMANCE ENHANCEMENT IN FERROELECTRIC THIN FILMS FOR UNCOOLED INFRARED IMAGING ARRAYS

July 1998

K.R. Udayakumar, H.R. Beratan, and C.M. Hanson
Raytheon Systems Company
Dallas, TX 75266

ABSTRACT

The development of high performance monolithic pyroelectric IR detectors requires ferroelectric films of high responsivity and high thermal isolation of self-supporting micromachined structures. In the DARPA-supported IR detector materials program, the ultimate goal is to demonstrate film properties that project to a system-level f/1 NETD of 10 mK for 48.5 µm-pixels. This paper will delineate materials and processes engineered towards that objective.

Films investigated in this program have been from the PLZT solid solution system. A sub-class of materials within this system, substituted with specific isovalent and donor elements, shows low projected NETDs, the lowest being 13.8 mK[1] for planar wafers. In general, addition of rare earth dopants has the dual effect of lowering the NETD and enhancing dc film resistivity (10^{12}-10^{14} Ω–cm) over 1-10 V. Room temperature film resistivity has been found to increase up to 10^{15} Ω–cm with a film thickness of 960 nm.

Processing studies indicate a general correlation among pyrolysis protocols, severity of RTA thermal budget and electrical performance. Furthermore, at film thicknesses of 150-350 nm, properties of films fabricated with a dilute precursor solution project thickness-modified NETDs lower than films with solution of higher molarity. Microstructural examination of rapid thermally annealed films, through transmission electron microscopy, reveal dense grains 36-43 nm in diameter with no evidence of second phase in the matrix or grain boundaries.

Experiments aimed primarily at investigating resistance degradation with electric field bias show that subjecting the films (350 nm-thick) to a prolonged high voltage bias (20 V for 8 hours, 40 V for 1 hour) before the standard poling procedure lead to material properties that project lower NETDs compared to films that underwent standard poling treatment without bias.

Lanthanum Strontium Cobalt Oxide, proposed as an alternate oxide transparent bottom electrode to the traditional metal electrodes, can be sputter-deposited at room temperature and then baked to yield film resistivity within the specified range of 1-150 mΩ-cm. A wet etch technique has been developed to pattern this oxide electrode that

[1] All NETDs in the paper to be modified by a factor of 0.77 to account for the sinusoidal wave form used in the model instead of the square wave form. All NETDs refer to the 48.5 µm pixels.

maintains physical integrity on rapid thermally processing. The baseline ferroelectric annealed at temperatures that ensure ROIC survivability predict NETDs of 26.4 mK.

1.0 INTRODUCTION

Raytheon's current generation of uncooled IR detectors is a hybrid technology, based on barium strontium titanate ceramic, operated near the phase transition, bump bonded to a readout IC, with organic mesas providing thermal isolation. These mesas are capable of thermal isolation of up to 1 MK/W, and the lowest NETD achieved has been about 38 mK (for 50 μm pixels). For a smaller pixel pitch, lower thermal conductance is required for higher performance, which is impossible with the current hybrid arrays. The next generation of uncooled IR detectors will thus implement monolithic technology employing ferroelectric films that offer a potential NETD of about 1 mK. The focus of this paper will be on the development of such IR materials. Salient features of the baseline ferroelectric will be delineated, following which methods of performance improvements will be described. Degradation studies initiated in advance of studies on ferroelectric films that operate under bias will then be briefly dealt with. The last section covers the deposition, patterning, and electro-physical characteristics of transparent bottom electrodes.

2.0 BASELINE FERROELECTRIC IMPROVEMENTS

The paper presented in the last symposium discussed in detail the MOD process for the fabrication of ferroelectric thin films, phase relations in the PLZT system, and material property measurements. The baseline ferroelectric chosen for the development of IR imaging arrays has a number of advantages. The precursor solution is extremely stable with long shelf life, and is suitable for manufacturing. The films have shown high performance at various pyrolysis and anneal protocols. In one study involving discontinuously pyrolyzed films (the films are ramped to intermediate temperatures and held there for 5 minutes to promote removal of organics) but anneals at thermal budgets ranging from 475°C/180 seconds to 700°C/10 seconds, property measurements projected NETDs within a narrow range of 19-25 mK. Particularly noteworthy is the ability to maintain sensitivity even at very low thermal budgets of 475°C/180 seconds and 500°C/30 seconds – thermal budgets that ensure the survival of ROICs.

2.1 Material Performance Variability

Person to person variability in the sensitivity of the films has been determined. Two technicians working independently fabricated the films, starting with the precursors, solution synthesis, spin-on fabrication, film anneals and took property measurements. Figure 1 represents the scatter plot of the projected NETDs for the 48.5 μm pixels; the test device IDs correspond to the different thermal conditions under which the films were processed. The two sets of data shown in the figure for each processing condition correspond to the data collected by the two technicians. The numerical values are incorporated, and the scale itself expanded to provide clarity and ease in reading the appropriate numbers. The average overall variation in projected NETDs is 2.5% between the 2 data sets, with the minimum and maximum variations being 0 and 9% respectively.

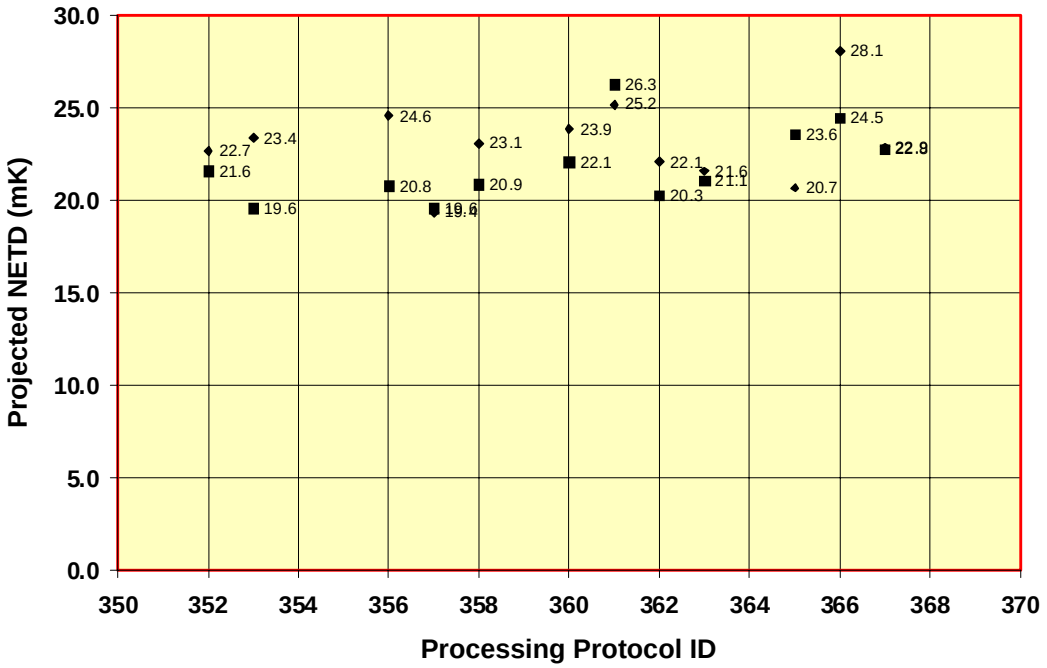

Figure 1. Person to person variability in projected NETDs for 48.5 micron pixel centers.

2.2 Solution Concentration

The final molarity of the spin-on solution appears to affect the properties of the film, and thus the figures of merit. Films were fabricated from solutions of concentrations 0.5 M and 0.125 M in the thickness range of 160 to 960 nm and annealed at 575°C/30 secs. For poling, a constant field of 275 kV/cm was maintained for all the thicknesses. Following evaluation of the dielectric and pyroelectric properties, projected NETDs were calculated which incorporated the actual thickness. At lower thickness levels (160-350 nm), for the same thickness, films fabricated with solution of lower concentration project lower NETDs by a factor of two. The projected NETDs for 0.16 μm and 0.28 μm films are 21 and 18 mK respectively. The contributing factor is the higher pyroelectric coefficient for the diluted solution; the pyroelectric coefficient for films with the 2 thicknesses corresponding to 0.5 M fall in the 7-8 nC/cm^2-K range, and that of 0.125 M solution in the 21-25 nC/cm^2-K range. Films of same thickness (0.16 μm) fabricated from both molarities that underwent microstructural examination through TEM failed to reveal any dramatic differences in grain sizes or phase relationships between the two. This is in spite of the fact that the films fabricated from the lower molarity encountered overall higher thermal budget compared to the higher molarity solution due to the number of layers increased by a factor of 4. Cross-section of the substrate/ buffer layers/ ferroelectric reveals that the various interfaces are sharp, except for the Pt/ferroelectric boundary which shows a slightly ragged edge. Only at very high magnifications does the micrograph indicate the possibility of Pt diffusing into the Ti layer; this has,

however, not been confirmed by micro-chemical analysis. The grain size of the ferroelectric along the longer diameter is about 43 nm, and 36 nm along the shorter diameter.

2.3 Effect Of Modification

Modification of the baseline ferroelectric took two forms. One involved substitution on the cation sites of the baseline ferroelectric and the second that of acceptor and donor dopant additions. Apart from the improvement in performance, rare earth element additives were designed to enhance the resistivity of the films (10^{12} to 10^{14} Ω-cm over a voltage range of 1-10 V). The most significant improvement in NETD resulted from cation substitutions, with the lowest NETD recorded being 13.8 mK. Plotted in Figure 2 are the iso-NETD contours for 48.5 μm pixels over which is superimposed the measured pyroelectric coefficients and permittivities of the modified formulations, processed under varying thermal protocols. It is clear that the modified baseline ferroelectric compositions predict NETDs that cluster around the 20 mK iso-NETD line. What is clear is also the fact that low permittivity, low tangent losses and moderately high pyroelectric coefficients typify the formulations.

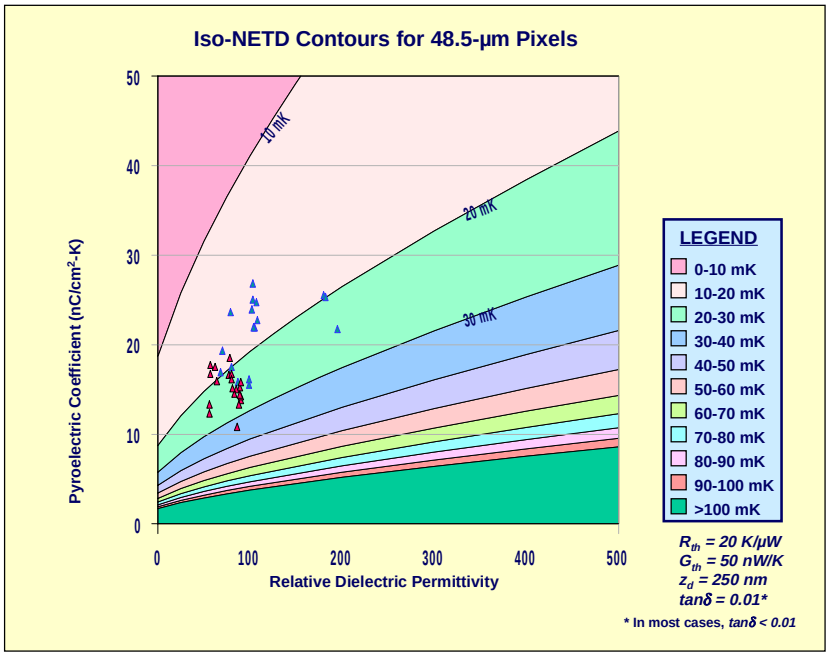

Figure 2. Lines of constant NETD juxtaposed with measured pyroelectric coefficients and dielectric permittivities for the modified baseline ferroelectric, for 48.5 μm pixels

2.4 Dielectric Degradation Experiments

As a prelude to investigating the performance of films that will operate near the phase transition, the baseline ferroelectric films were subjected to prolonged high voltage dc bias to determine the breakdown regime. Typically, three regions before the onset of total breakdown have characterized the I-

V behavior of ferroelectric films. We have observed the "soak time", in which the charging current includes the charging current from the dielectric, ferroelectric polarization and the build-up conductance, generally involving a relaxation in current with time. The second region, that corresponds to the "leakage current", remains steady with time, and accrues from conduction due to ohmic, ionic, space charge, tunneling and Poole-Frenkel emission; our data has hitherto been confined up to this region. The third region is the "electrical degradation" region which has been variously rationalized in the literature through grain boundary model, reduction model, potential barrier height reduction model and de-mixing model; in this region, current rises with time, leading eventually to breakdown. The breakdown current has been assigned empirically to be an order of magnitude higher than the steady current in the leakage current regime. To assess the breakdown in the films, a 20 V dc bias was applied and the current monitored as a function of time. This voltage being higher than the threshold voltage, current rose with time. Starting with 2.4 μA, a current of 2.8 μA was recorded in 80 seconds, following which it increased dramatically to 169 μA, and remained constant until the experiment was aborted after 8 hours, when the current read 170 μA. In this process, the dissipation loss increased from 2.1% to 11%. The films were then poled and the properties measured; tangent loss recovered to 1.5%, with a dielectric permittivity of 60 and pyroelectric coefficient of 20.2 nC/cm^2-K, which project to an NETD of 16.4 mK. With a similar procedure for 40 V dc bias held for an hour, the projected NETD is 16 mK. When the pads were not poled in the standard routine after subjecting to a 40 V dc bias, and pyroelectric coefficients measured, the projected NETD was higher (87 mK). Thus, the films have to be poled after subjecting to high voltage bias to realize low projected NETDs. Films when tested under standard conditions - no high voltage bias before poling – were privy to material properties that project to an NETD of 21.5 mK. Clearly, the projected NETDs were better with films subjected to a high voltage bias before the standard poling treatment.

3.0 TRANSPARENT OXIDE BOTTOM ELECTRODE

In the current design of building monolithic structures, the ferroelectric film is sandwiched between metal electrodes, and for the 250 nm-thick ferroelectric film, the absorption efficiency for IR radiation is low (15 to 25%). To increase the absorption efficiency, an alternate absorption cavity design involves establishing a quarter wave resonant cavity between the top electrode and a reflective layer on the ROIC. That mandates a highly transparent bottom electrode. For a practical implementation of this scheme, the sheet resistance of the bottom electrode must be sufficiently low to avoid an adverse electrical impact on signal and noise, and sufficiently high to avoid reflection of IR radiation; the acceptable range of resistivity is about 0.001 to 0.15 Ω-cm for a 25 nm-thick film.

3.1 Film Resistivity

Films of lanthanum strontium cobalt oxide (LSCO) were deposited in an MRC 603 sputtering system at ambient temperature. Four-point probe measurements showed the as-deposited films to be highly resistive, with a sheet resistance of greater than 10^6 Ω/square. The films were "baked" (as distinct from "annealed", implying film crystallization) at various temperatures and dwell times to lower the sheet resistance, both through furnace and rapid thermal annealing. As evident in Figure 3, the sheet resistance decreases with the severity of RTA thermal budget; a similar trend has been noticed with furnace baked films. Calculations of sheet resistivities reveal that the thermal budgets that can be realistically used for building thermally isolated structures on ROICs are limited by two factors. First, thermal budgets in excess of that corresponding to 600°C/10 seconds damage the ICs on which the

structures are built; and second, thermal budgets with a severity gentler than 550°C/30 secs pushes the film resistivities to beyond the maximum allowable resistivity range. This, consequently, confines the thermal treatment to a RTA temperature of 550°C with dwell times of 30 to 180 seconds.

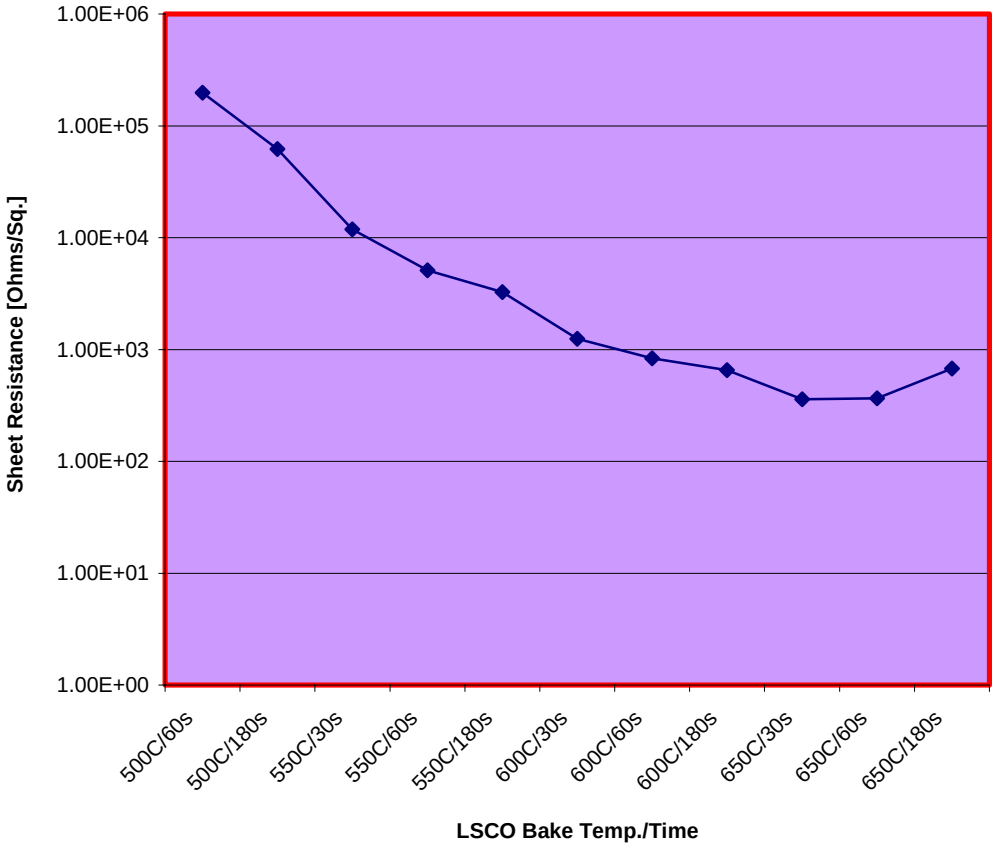

Figure 3. Sheet resistance plotted as a function of LSCO bake temperature/time (rapid thermally processed). Note the fall in sheet resistance with severity of annealing

3.2 LSCO Patterning

Closely linked to the material performance is the ability to build free-standing structures through conventional silicon processing techniques. Wet etch chemicals employed for this purpose included the ferroelectric etchant (a mixture of buffered oxide etch, HCl and deionized H_2O in the ratio 1:2:3), aluminum leach, CR7 chromium etchant and hydrogen peroxide. The effect of ferroelectric etchant was studied in some detail by attempting to pattern and etch the bottom electrode structure. In Figure 4 is shown the path towards an optimum etching time - 5 seconds being too short (under etch), 12 seconds being too long (over etch), with 6 seconds being the optimum etch time. For a better control of the etch time, the concentration of the etchant has been lowered; with the diluted solution, a 120 nm-thick LSCO film is etched in 50 seconds. Aluminum leach etchant, predominantly constituted of phosphoric acid and

acetic acid, etches well for planar LSCO, but does not maintain arm integrity for the finer geometries used in the building of thermal isolation structures. LSCO films are patterned before the bake; baking a full sheet of LSCO, without patterning, results in film peeling.

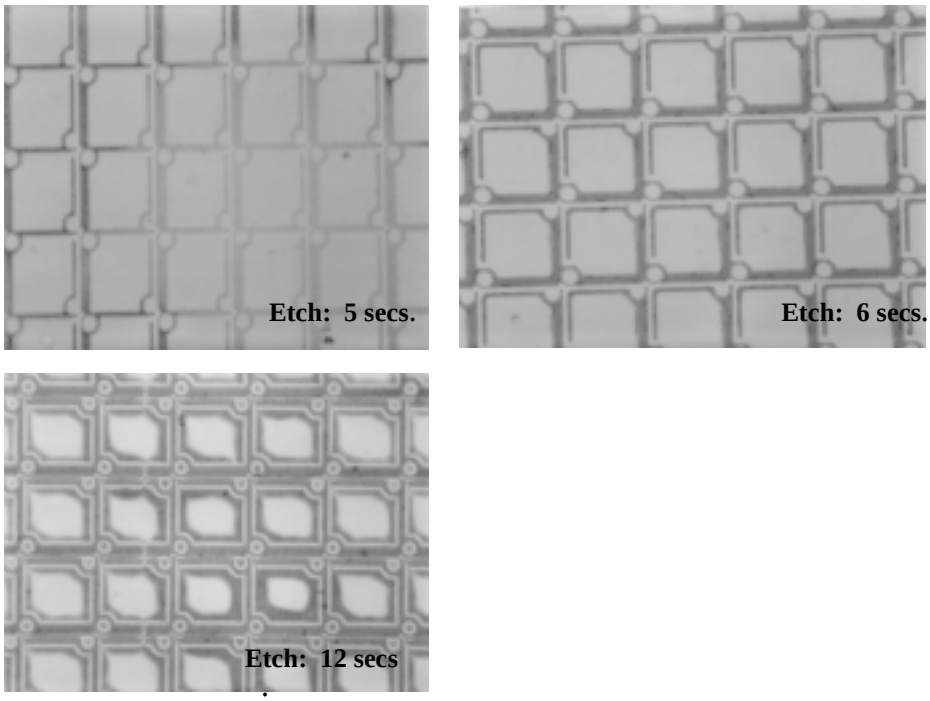

Figure 4. Micrographs of patterned LSCO bottom electrode at varying etch times: 5 seconds (under etch), 6 seconds (optimum), and 12 seconds (over etch)

3.3 Electrical Characteristics

To evaluate the film performance with LSCO bottom electrode, ferroelectric films were grown on 33 nm-thick LSCO. The films were rapid thermally annealed at thermal budgets compatible with the survival of the ROICs. From the dielectric and pyroelectric measurements, projected NETDs were in the range of 50-100 mK, for 48.5 μm pixels. The relatively higher projected NETD with LSCO bottom electrode, compared to that of Pt arises mainly from the higher dissipation losses. High frequency dielectric measurements have shown dispersion in capacitance and dielectric loss factor. Typically, the tangent loss increases with frequency, attaining a peak, and then decreases with further increase in frequency; the film permittivity falls with frequency. This is in contrast to the film behavior with Pt bottom electrode in which the dielectric permittivity and loss factor of the ferroelectric are stable over a wider frequency range.

A number of electrode/ ferroelectric/ electrode configurations and processing conditions have been employed to obtain a better understanding of the transparent electrode. From the results obtained to date, the best projected NETDs have been for a configuration with platinized wafers on which 33 nm-thick LSCO is sputter deposited (Si/SiO2/Ti-Pt/LSCO/ferroelectric). Baking of LSCO and anneal of the

ferroelectric with either the conventional furnace or RTA have both yielded low NETDs. In both cases, the capacitance and tangent loss have been non-dispersive with frequency. From the electrical measurements, the RTAed films (LSCO baked at 550°C/60 seconds and the ferroelectric annealed at 500°C/180 seconds) had a projected NETD of 26.2 mK (for 48.5 μm pixels). The conventional furnace baked and annealed films (LSCO at 500°C/30 minutes, and ferroelectric at 650°C/15 minutes) had a projected NETD of 52.1 mK (for 48.5 μm pixels).

Electrical performance results of ferroelectric films reported in the preceding, with LSCO bottom electrode, were based on an electrode thickness of 33 nm; contacts to the oxide electrode were typically reinforced with silver epoxy paste. Film characteristics have also been examined on 110 nm-thick LSCO films sputter deposited on oxidized silicon. Ferroelectric films were processed under all three pyrolysis conditions (instant, continuous, and discontinuous), followed by rapid thermal annealing at 500°C/180 seconds. Instant pyrolysis refers to films being subjected to the final temperature without a ramp; continuous pyrolysis refers to films being ramped to the final temperature; and, discontinuous pyrolysis refers to films being ramped to intermediate temperatures and soaked for a specified time. Discontinuously pyrolyzed films showed the highest pyroelectric coefficient of 19.1 nC/cm^{2}K, with dielectric permittivity and dissipation losses of 160 and 0.051 respectively at 1 kHz, which projects to an NETD of 42.2 mK. A lower tangent loss of 2.1% and permittivity of 100 at 100 Hz frequency leads to a projected NETD of 23.6 mK. Films pyrolyzed through the "instant pyrolysis" route had the lowest pyroelectric coefficient of 5.5 nC/cm^{2}K. "Continuously" pyrolyzed films show an intermediate performance of 60.5 mK and 51.7 mK based on dielectric properties measured at 1 kHz and 100 Hz respectively.

Current-time measurements were taken on the ferroelectric with 30 nm-thick LSCO bottom electrode, reinforced with conductive silver paste, to assess the dc resistivity, employing a Keithley electrometer. DC biases of 1 and 5 Volts were employed (Figure 5). For the device-relevant bias of 1 V, the saturation current was 32 pA; for the 0.38 μm-thick film and 1 mm-diameter pad used in collecting the data, this corresponds to a resistivity of $3x10^{12}$ Ω-cm.

3.4 Microstrutural Analysis

Analytical scanning (SEM) and transmission electron microscopy (TEM) examined typical samples, which have been used for electrical testing. The samples for analysis were mounted and fractured in a Hitachi S800 field emission SEM and examined in the back scattered (BSE) and secondary electron (SE) modes at an accelerating voltage of 20 kV. Wafers were thinned in a direction perpendicular to the coating layers using a focussed ion beam (FIB); these thinned samples were examined in a JEOL 1200EX TEM operating at 100 kV. From Figure 6, at least four different layers can be seen. Each layer is delineated with arrows in the figure, which is a TEM bright field image of the cross section of the wafer. As annotated in the figure, the outermost two layers are platinum layers (sputtered and FIB deposited) to protect and define the outer edge of the sample. The thicknesses of each of the layers, as determined from Figure 6, are 330 nm of LSCO; ferroelectric layers of 120, 150 and 120 nm, amounting to a total thickness of 420 nm. The microstructure shows a clear demarcation between LSCO and the ferroelectric, with no visible physical interdiffusion between the layers. The layers L2-L4 in the micrographs correspond to the three layers constituting the ferroelectric film.

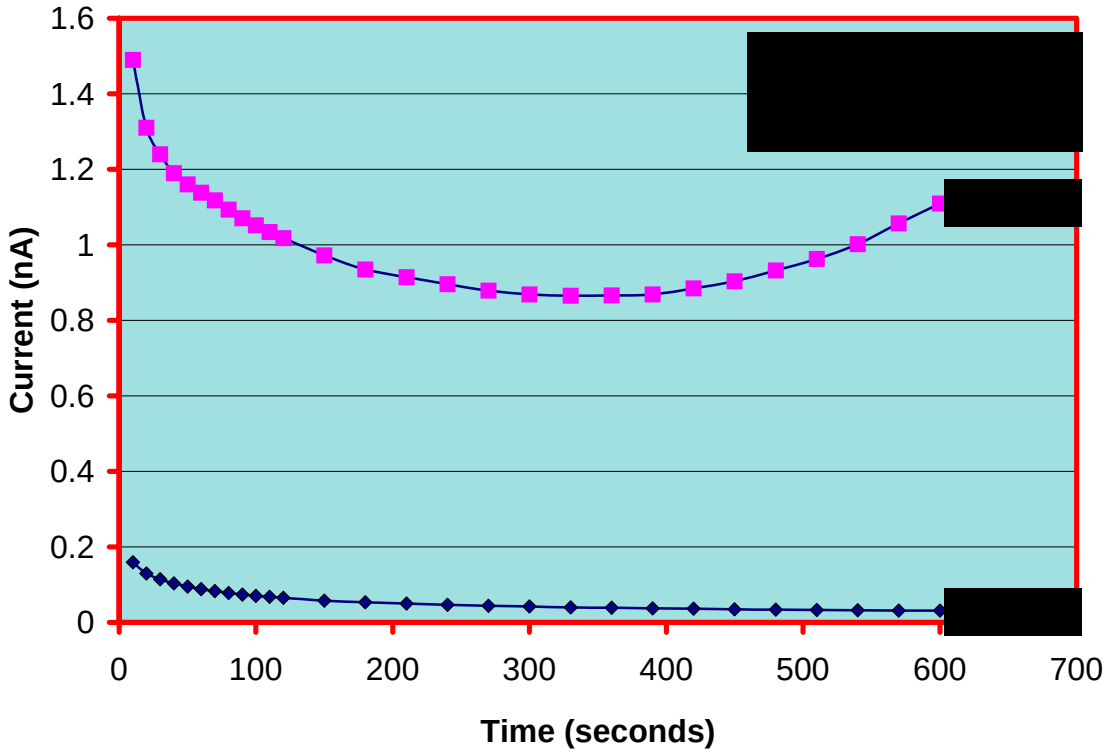

Figure 5. Current-time plot for the baseline ferroelectric film with LSCO bottom electrode (30 nm-thick) at varying dc bias

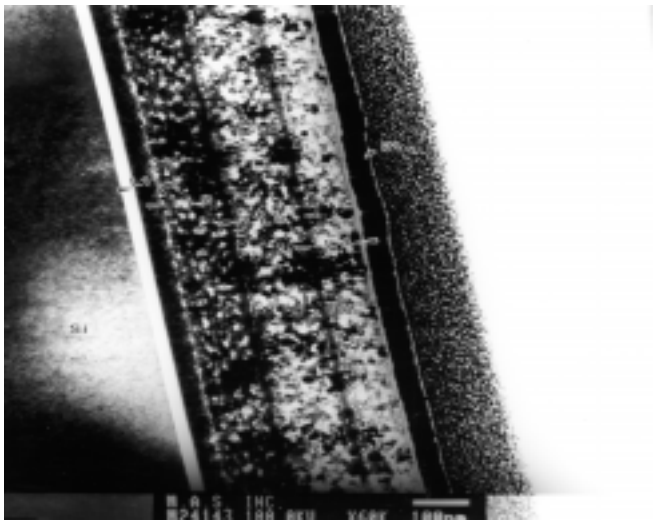

Figure 6. Cross-sectional transmission electron micrograph showing the oxide electrode/ silicon dioxide and oxide electrode/ferroelectric interface. The actual magnification is 160,000X.

4.0 SUMMARY

The characteristics described in this paper have been for ferroelectric films that operate in the pyroelectric mode, far below the phase transition. Experiments have been planned for the study of films that operate near the phase transition and under bias. For the present, the baseline ferroelectric is being used in the development of 320x240 IR imaging arrays, and in the development of 25 nm-thick top and bottom transparent oxide electrodes. As evident, the baseline ferroelectric is distinguished by high performance even at low crystallization temperatures, low operator to operator variability, improved performance with elemental modifications, and stability under high voltage stress. From the film properties of both the baseline ferroelectric and its modification, the lowest predicted system-level f/1 NETD has been 13.8 mK. It has been possible to sputter-deposit LSCO at room temperature and then bake the films to obtain film resistivities within the desired range. The films could be patterned with a wet etch technique without compromising on the film integrity even for finer geometries. With the oxide bottom electrode, film properties project to an NETD of 23.6 mK.

We thank Ray Balcerak, Jim Miller, Bill Clark, and Bob Hoffman for their support to pursue these developments. We thank Jerome Woody, Tony Owens, and Bruce Moss, the technicians who were instrumental in doing the actual work reported in this paper.